#### PRIMARY RESEARCH ARTICLE



# Phosphorus rather than nitrogen regulates ecosystem carbon dynamics after permafrost thaw

Guibiao Yang<sup>1,2</sup> | Yunfeng Peng<sup>1</sup> | Benjamin W. Abbott<sup>3</sup> | Christina Biasi<sup>4</sup> | Bin Wei<sup>1,2</sup> | Dianye Zhang<sup>1</sup> | Jun Wang<sup>1</sup> | Jianchun Yu<sup>1</sup> | Fei Li<sup>1</sup> | Guanqin Wang<sup>1,2</sup> | Dan Kou<sup>1,4</sup> | Futing Liu<sup>1</sup> | Yuanhe Yang<sup>1,2</sup> |

### Correspondence

Yuanhe Yang, State Key Laboratory of Vegetation and Environmental Change, Institute of Botany, Chinese Academy of Sciences, Beijing 100093, China. Email: yhyang@ibcas.ac.cn

### Funding information

National Natural Science Foundation of China, Grant/Award Number: 31825006, 31988102 and 91837312; Second Tibetan Plateau Scientific Expedition and Research, Grant/Award Number: 2019QZKK0106; Key Research Program of Frontier Sciences, Chinese Academy of Sciences, Grant/Award Number: QYZDB-SSW-SMC049; China National Postdoctoral Program for Innovative Talents, Grant/Award Number: BX20200363

#### **Abstract**

Ecosystem carbon (C) dynamics after permafrost thaw depends on more than just climate change since soil nutrient status may also impact ecosystem C balance. It has been advocated that nitrogen (N) release upon permafrost thaw could promote plant growth and thus offset soil C loss. However, compared with the widely accepted C-N interactions, little is known about the potential role of soil phosphorus (P) availability. We combined 3-year field observations along a thaw sequence (constituted by four thaw stages, i.e., non-collapse and 5, 14, and 22 years since collapse) with an in-situ fertilization experiment (included N and P additions at the level of 10 g N m<sup>-2</sup> year<sup>-1</sup> and 10 g P m<sup>-2</sup> year<sup>-1</sup>) to evaluate ecosystem C-nutrient interactions upon permafrost thaw. We found that changes in soil P availability rather than N availability played an important role in regulating gross primary productivity and net ecosystem productivity along the thaw sequence. The fertilization experiment confirmed that P addition had stronger effects on plant growth than N addition in this permafrost ecosystem. These two lines of evidence highlight the crucial role of soil P availability in altering the trajectory of permafrost C cycle under climate warming.

#### KEYWORDS

carbon cycle, carbon fluxes, carbon-climate feedback, climate warming, nutrient availability, thermokarst

## 1 | INTRODUCTION

Ecosystems underlain by permafrost store more than half of global soil organic carbon (SOC), approximately twice the atmospheric carbon (C) pool (Hugelius et al., 2014; Mishra et al., 2021). In the last two decades, permafrost regions have experienced two times faster warming than the global mean (Meredith et al., 2019), triggering widespread permafrost thaw (Brown & Romanovsky, 2008;

Chadburn et al., 2017). After thawing, microorganisms can accelerate the decomposition of soil organic matter, and produce carbon dioxide ( $CO_2$ ) and methane ( $CH_4$ ), which could lead to a positive C feedback to climate change (Schuur et al., 2015; Turetsky et al., 2019, 2020; Walter Anthony et al., 2018). Meanwhile, both the enhanced microbial decomposition and thawing of permafrost layer would release considerable amounts of nutrients (Finger et al., 2016; Keuper et al., 2017; Mao et al., 2020; Salmon et al., 2016). The improved

<sup>&</sup>lt;sup>1</sup>State Key Laboratory of Vegetation and Environmental Change, Institute of Botany, Chinese Academy of Sciences, Beijing, China

<sup>&</sup>lt;sup>2</sup>University of Chinese Academy of Sciences, Beijing, China

<sup>&</sup>lt;sup>3</sup>Department of Plant and Wildlife Sciences, Brigham Young University, Provo, Utah, USA

<sup>&</sup>lt;sup>4</sup>Department of Environmental and Biological Sciences, University of Eastern Finland, Kuopio, Finland

soil nutrient status is conducive to plant growth and vegetation C fixation, which could partly offset soil C loss driven by permafrost thaw (Christiansen et al., 2018; Keuper et al., 2017; Kicklighter et al., 2019). Therefore, an in-depth understanding of changes in soil nutrient status after permafrost thaw and their effects on ecosystem C exchange is crucial for accurately predicting the trajectory of permafrost C cycle under climate warming.

Due to the important role of soil nutrients in regulating permafrost C cycle, the global change research community has increasingly focused on changes in soil nutrient status upon permafrost thaw and their subsequent effects (Finger et al., 2016; Keuper et al., 2017; Pedersen et al., 2020). It has been reported that permafrost thaw could lead to an increase in soil nitrogen (N) availability, subsequently stimulating plant growth and ecosystem C uptake (Christiansen et al., 2018; Finger et al., 2016; Keuper et al., 2017; Salmon et al., 2016). Increased plant productivity has been projected to counterbalance soil C loss through the 21st century (McGuire et al., 2018). However, these model simulations are not consistent with field measurements which advocate that permafrost ecosystems could function as a significant C source due to the higher C loss during the shoulder and winter seasons (Commane et al., 2017; Natali et al., 2019; Parazoo et al., 2016). This data-model mismatch may be partly due to the limited consideration of nutrient constraint on vegetation growth among Earth system models (Wieder et al., 2015). Soil phosphorus (P), apart from N, is another key limiting macronutrient for plant growth. Generally, the higher soil P availability can stimulate plant P uptake and thus tissue P concentrations, which is also beneficial for net photosynthetic rate, plant growth rate, and vegetation C fixation (Reich et al., 2009; Wieder et al., 2015). Considering that vegetation P limitation is pervasive in terrestrial ecosystems (Hou et al., 2020: Peñuelas et al., 2013; Vitousek et al., 2010), it is thus necessary to consider both soil N and P availability when examining C-nutrient interactions after permafrost thaw (Street et al., 2018). However, compared with the increasingly recognized C-N interactions, it remains unknown whether and how thaw-induced changes in soil P status affect C cycling processes in permafrost ecosystems.

The Tibetan Plateau is the largest alpine permafrost region around the world, representing approximately three-quarters of global alpine permafrost (Wang & French, 1995). Similar to other permafrost regions, the plateau owns a high soil C density (C amount per area), especially in alpine swamp meadow (Ding et al., 2016), and has experienced pronounced warming and permafrost thaw in recent decades (Wang et al., 2008; Wu & Zhang, 2008), which could induce potential soil C emissions (Chen et al., 2016; Li, Peng, Chen, et al., 2019). Up to now, some studies have examined the effects of experimental warming and permafrost thaw on SOC stock and its molecular composition as well as ecosystem C fluxes on the Tibetan Plateau (Li, Peng, Chen, et al., 2019; Liu et al., 2018; Mu et al., 2017). Yet, less study has addressed the role of soil nutrient in regulating ecosystem C fluxes across the Tibetan alpine permafrost region. In this study, we examined the potential roles of soil N and P availability in regulating ecosystem C cycle along a permafrost thaw sequence on the Tibetan Plateau. Specifically, we monitored ecosystem C

fluxes (including gross primary productivity, net ecosystem productivity, and ecosystem respiration; hereafter referred as GPP, NEP, and ER, respectively), and determined soil N and P availability along the thaw sequence. Given that permafrost thaw can also trigger ecosystem C dynamics by altering soil temperature, moisture, and plant properties (Finger et al., 2016; Keuper et al., 2017), we quantified various abiotic factors (soil temperature and moisture) and biotic factors (leaf N and P concentrations, leaf area index [LAI], and the relative abundance of forb) to gain a comprehensive understanding on dominant drivers of ecosystem C fluxes along the thaw sequence. To verify the potential role of soil nutrient availability in modulating ecosystem C dynamics observed along the thaw sequence, we performed an in-situ fertilization experiment and explored changes in ecosystem C fluxes, the normalized difference vegetation index (NDVI), and aboveground biomass (AGB) after nutrient additions. Based on these measurements, this study aimed to (1) examine how ecosystem C fluxes and soil nutrient availability would change along the thaw sequence and (2) determine what roles of soil N and P status would play in regulating ecosystem C fluxes after permafrost thaw. We hypothesize that soil N and P availability could increase upon permafrost thaw, and both of them would promote plant growth and enhance ecosystem C uptake.

#### 2 | MATERIALS AND METHODS

### 2.1 | Site description

The study site is located in the northeastern Tibetan Plateau (N 37°28′, E 100°17′, altitude ~3900 m, average active layer thickness ~0.9 m), which is one of the five typical permafrost zones on the plateau (Jin et al., 2011). This site has a mean annual temperature of -3.3°C and a mean annual precipitation of 460 mm. The grassland type is alpine swamp meadow, and the vegetation community is mainly composed of two functional groups: sedge (Kobresia tibetica Maxim., Kobresia royleana (Nees) Bocklr. and Carex atrofusca subsp. minor (Boott) T. Koyama) and forb (Triglochin maritimum L., Saussurea pulchra Lipsch. and Potentilla saundersiana Royle, etc.). The permafrost thaw feature in this area belongs to thermo-erosion gully (Kokelj & Jorgenson, 2013). Before permafrost thaw, the study area is relatively homogeneous (see Text S1 for details). Permafrost has progressively collapsed upslope during the past 25 years, creating a thaw sequence with the most recent collapse landscapes occurring near the gully head (Figure S1a).

# 2.2 | Measurements of CO<sub>2</sub> flux and associated drivers along the thaw sequence

We established four plots (each plot with an area of  $15 \times 20 \text{ m}^2$ ) along the thaw sequence mentioned above, one in uncollapsed grassland area and three in collapsed area. The plot in uncollapsed grassland area served as control and the other three plots were dispersed at

intervals of ~80 m along the thaw sequence, representing different thaw stages (early, middle, and late thaw stage, Figure S1b-e). The time since collapse was estimated at 5, 14, and 22 years prior to 2017 based on the ratio of the distance between the gully head and each plot to the rate of gully retreat (see the detailed information in Yang, Peng, Marushchak, et al., 2018; Yang, Peng, Olefeldt, et al., 2018). All plots were enclosed with fences to prevent animal grazing before CO<sub>2</sub> flux measurements. Within each experimental plot, thermokarst formation tore apart the grassland landscape into numerous vegetated rafts with different area (the mean area of 4.5 m<sup>2</sup>; Figure S1). The heterogeneous microenvironments could result in the relatively independent properties among vegetated rafts, which were proved by the later spatial autocorrelation analyses (e.g., GPP and soil nutrient availability; Table S1). Due to this, we randomly chose 10 vegetated rafts within each plot as replicates, and then inserted a plastic ring with 26 cm diameter and 12 cm high into the soil at a 10 cm depth in each vegetated raft.

To evaluate changes in ecosystem C exchange along the thaw sequence, we measured GPP, NEP, and ER using static chamber method (Li et al., 2017; Natali et al., 2014). Specifically, NEP was measured with an infrared gas analyzer (IRGA, LI-6400, LiCor Inc.) attached to a transparent static chamber (26 cm diameter and 40 cm high), which was equipped with a small electric fan to promote the mixture of the headspace air within the chamber. The chamber was sealed into a water-filled groove at the top of the plastic ring before each measurement. CO2 concentration in the chamber was then measured for 1.5 min at 10 s intervals after an equilibration period (~10 s) to ensure that the CO<sub>2</sub> concentration increased or decreased steadily over time. After each measurement, the chamber was lifted and vented to recover CO2 concentration to the ambient level. NEP was determined as the slope of the linear relationship between CO<sub>2</sub> concentration and measurement time, with negative values referring to ecosystem C uptake from the atmosphere and vice versa. After NEP measurements, ER was immediately determined using the same procedure by covering the chamber with an opaque cloth to block all light. Finally, we calculated GPP as the difference between ER and NEP. Notably, we mainly focused on ecosystem C fluxes during the peak growing season since this study aimed to evaluate changes in ecosystem C exchange among different thaw stages. Moreover, to ensure that changes in ecosystem C fluxes among different thaw stages were coincident within the whole growing season, we determined the seasonal dynamics of CO2 flux in 2018. Overall, ecosystem C exchange was measured every 10-15 days between 9:00 am and 12:00 pm (local time) from July to September in 2017 and May to October in 2018, and 17th July and 3rd August 2019.

To explain variations in  $\mathrm{CO}_2$  fluxes along the thaw sequence, we also measured NDVI inside each ring with an ADC multi-spectral digital camera (Tetracam) during  $\mathrm{CO}_2$  flux measurements, and recorded soil temperature and moisture in the top 10 cm with a digital thermometer and a portable TDR-100 soil moisture probe (Spectrum Technologies Inc.), respectively. In addition, we determined biotic factors (LAI, the relative abundance of forb, and leaf N and P concentrations) in 2018. LAI was estimated following a well-established

protocol (Shaver et al., 2007). Specifically, we first determined NDVI in five quadrats ( $10 \times 10 \text{ cm}^2$ ) distributed along the thaw sequence. Of these five quadrats, two were located at the control site, and three were distributed at three thaw stages, respectively. We then collected all leaves within each quadrat, and determined leaf area using a scanner (LIDE-300, Canon) combined with WinRhizo software (Regent Instruments Inc.). LAI was further calculated by dividing leaf area with the quadrat area. In each measurement, both LAI and NDVI were obtained in five pairs from the five quadrats mentioned above. The measurements were conducted three times every month from June to August in 2018. In total, we obtained 45 paired measurements of LAI and NDVI (5 pairs in each measurement  $\times$  3 times per month  $\times$  3 months) to establish their relationship ( $R^2 = 0.86$ , p < 0.001) as follows:

$$LAI = 0.21e^{4.49NDVI}.$$
 (1)

Based on this empirical equation, LAI in the plastic rings was then calculated using the corresponding NDVI determined during CO<sub>2</sub> flux measurement.

At the end of July in 2018, we investigated plant species composition, then estimated the relative abundance of forb within each plastic ring. After that, we collected green leaves for the whole aboveground vegetation for elemental analysis. The collected samples were dried to constant weight at 60°C, ground and sieved to analyze leaf N and P concentrations. Of them, leaf N concentration was analyzed by an elemental analyzer (Vario EL III; Elementar Inc.), and leaf P concentration was determined after digestion with  $\rm H_2SO_4$  and  $\rm H_2O_2$  at 380°C for ~3 h following the vanado-molybdate method with a spectrophotometer (UV-2550; Shimadzu).

# 2.3 | Measurements of soil N and P availability and associated drivers along the thaw sequence

To evaluate the potential roles of soil nutrient availability in regulating ecosystem C dynamics along the thaw sequence, we measured inorganic N and P concentrations in soil extracts and solution as well as soil N and P mineralization rates during the peak growing season. As revealed by an additional <sup>15</sup>N trace study, plant-available nutrients mainly stemmed from the topsoil rather than the subsoil at our study site (see Text S2 for details). We thus focused on the effects of topsoil nutrient availability on ecosystem C fluxes upon permafrost thaw. Specifically, we measured inorganic N and P concentrations in soil extracts, inorganic N and P concentrations in soil solution, and soil N and P mineralization rates. To do so, we collected three soil cores near each plastic ring at the end of July 2018 using a 2.5 cm (inside-diameter) auger to a 15 cm depth, and then mixed them to obtain one composite sample for each vegetated raft. The composite soil samples were handpicked to remove all roots and gravels, sieved through a 2 mm mesh, and then divided into two parts. One part was immediately cooled at 4°C, and the other part was air dried. The subsample stored at 4°C was extracted with 1 M KCl solution, and then

analyzed using a flow injection analyzer (Autoanalyzer 3 SEAL, Bran and Luebbe) for  $\mathrm{NH_4}^+\text{-}\mathrm{N}$  and  $\mathrm{NO_3}^-\text{-}\mathrm{N}$  concentrations. Air-dried soils were extracted with 0.03 M  $\mathrm{NH_4F}$  and 0.025 M HCl, and analyzed colorimetrically to determine extractable P concentrations using vanado-molybdate method (Bray & Kurtz, 1945). Beside analyzing soil samples, soil pore water was collected at a depth of 10 cm every month from June to September in 2018, and immediately filtered and stored at -20°C. Samples were transported to indoor laboratory and analyzed using a flow injection analyzer for  $\mathrm{NH_4}^+\text{-}\mathrm{N}$ ,  $\mathrm{NO_3}^-\text{-}\mathrm{N}$ , and inorganic P concentrations.

Soil N and P mineralization rates were determined using field incubations conducted for two consecutive periods from mid-July to mid-August and from mid-August to mid-September in 2018 (Edwards et al., 2015). Specifically, a plastic tube with 5 cm diameter was inserted to a depth of 10 cm within each of 10 vegetated rafts selected in this study. After that, all the vegetation within the tube was clipped, and the tube was pulled out to cover its bottom with a nylon mesh bag containing ~5 g ion-exchange resin. The resin bag was shaken in 2 M KCl solution for 3 h to saturate exchange sites with K<sup>+</sup> and Cl<sup>-</sup> ions, washed with distilled water and then dried at 60°C before the installation. The tube covered with resin bag was then put back to its original location, and the soil at the same depth were sampled near the plastic tube. After 1-month incubation, the resin bag was removed and rinsed with deionized water, and soil within the tube was collected. Both the soil samples and resin bags were brought back to the laboratory, stored at -20°C and extracted with 1 M KCl solution at the room temperature. The extracted liquids were analyzed for inorganic N (NH<sub>4</sub><sup>+</sup>-N and NO<sub>3</sub><sup>-</sup>-N) and inorganic P concentrations. Finally, soil N or P mineralization rate was calculated as the difference of the post-incubated amount of inorganic N (NH<sub>4</sub><sup>+</sup>-N and NO<sub>3</sub><sup>-</sup>-N) or inorganic P in soils and resin bags with the corresponding values in soils before incubation, and expressed on the basis of the bottom area of plastic tube and the incubated time  $(ng cm^{-2} day^{-1}).$ 

To explore potential drivers of soil nutrient availability along the thaw sequence, we measured biotic and abiotic factors in the surface soil, including soil and root surface acid phosphatase, soil pH, clay content, and metal minerals. Of them, soil and root surface acid phosphatase were determined using fluorometric techniques (Deng et al., 2016; Marx et al., 2001). Briefly, soil samples and live roots were collected at the end of July in 2018 and immediately transported to the laboratory. Soil samples (~2.75 g) were mixed with 91 ml 50 mM sodium acetate buffer, stirred for 2 min. Accordingly, root samples (~100 mg) were washed with deionized water to remove the rhizosphere soil, amended with 9 ml of 50 mM sodium acetate, sonicated for 2 min and shaken for 1 h. After these treatments, 170  $\mu$ l of the extracting solution of soil samples or live roots and 50 μl of 200 μM hydrolysis of the methylumbelliferone (MUB)-phosphate were pipetted into the microplate with 16 replicates and incubated for 2 h at 25°C in the dark. Meanwhile, 170 µl of extracting solution of soil samples or live roots and 50  $\mu$ l of standards (0 to 50  $\mu$ M MUB) were incorporated into the microplate with 16 replicates and incubated for 2 h at 25°C in the dark to produce a standard curve. The reaction was terminated by adding 10  $\mu$ l of 1 M NaOH. Fluorescence of the MUB was quantified using a fluorometric spectrometer (Beckman Coulter DTX 880) equipped with a near-UV lamp, 365 nm excitation, and 450 nm emission. Finally, soil and root surface acid phosphatase (nmol g<sup>-1</sup> h<sup>-1</sup>) were determined by the fluorescence of measured samples and the standard curve mentioned above.

Soil pH was determined in a 1:5 soil-to-deionized water suspension using a pH probe (PB-10, Sartorius), and soil texture was measured using a particle size analyzer (Malvern Masterizer 2000) after removing organic matter and carbonates using 30% hydrogen peroxide and 30% hydrochloric acid. We also measured three forms of Fe/Al-(hydr) oxides according to Lalonde et al. (2012), including free Fe-(hydr) oxides (Fe<sub>d</sub>), amorphous Fe/Al-(hydr) oxides (Fe<sub>o</sub> + Al<sub>o</sub>), and complexed Fe/Al-(hydr) oxides (Fe $_{\rm p}$  + Al $_{\rm p}$ ). Of them, Fe $_{\rm d}$  was extracted using a mixed solution consisting of 0.1 M sodium dithionite, 0.27 M trisodium citrate, and 0.11 M sodium bicarbonate after continually stirring the soil solution in the 80°C water bath for 15 min (Lalonde et al., 2012).  $Fe_0 + Al_0$  and  $Fe_p + Al_p$  were extracted by 0.2 M oxalic acid-ammonium oxalate (pH = 3) and 0.2 M sodium pyrophosphate after shaking the soil solution in the dark for 4 h, respectively (Keiluweit et al., 2015). The supernatants were centrifuged for element measurements. All three forms of Fe/Al-(hydr) oxide contents were determined with an inductively coupled plasma-optical emission spectrometer (iCAP 6300. Thermo Scientific).

### 2.4 | Fertilization experiment

To test nutrient effects on ecosystem C fluxes observed along the thaw sequence, we set up a fertilization experiment in the uncollapsed grassland area in May 2019. The experiment included three treatments: control, N, and P additions, with four replicates being assigned to each treatment using a completely randomized design. Notably, the treatment of N + P addition which could investigate the interaction of these two elements was not included in our experiment and the fertilization experiment was only performed in the control site, since this additional experiment was mainly designed to compare the individual effect of N or P availability on plant growth, and to verify whether N or P was the restrictive element for plant growth across our study area. There were 12 plots  $(1 \times 1 \text{ m}^2)$  in total, separated by at least 1.5 m between two adjacent plots as a buffer zone. N and P were applied at 10 g N m<sup>-2</sup> year<sup>-1</sup> and 10 g P m<sup>-2</sup> year<sup>-1</sup>, respectively. This was enough for plant-growth requirement, being about 12 times for N requirement and 148 times for P requirement (Chapin et al., 1995; Shaver & Iii, 1991). Meanwhile, given that N may be more easily leached compared to P (Norberg & Aronsson, 2020), N fertilizer, in the form of ammonium nitrate, was applied two times in 30th May and 3rd July, 2019, and P fertilizer, in the form of triple super phosphate, was added once in 30th May 2019. Based on this fertilization experiment, we measured ecosystem C fluxes and NDVI using the same approaches as those used along the thermoerosion gully. AGB was determined in late August 2019 by clipping  $25 \times 25$  cm<sup>2</sup> quadrat and oven-drying to constant weight (48 h at 60°C). In addition, we collected plant and soil samples in 15th July 2019, so as to measure leaf N, P and soil inorganic N, P concentrations using the same approach mentioned above.

To understand the potential differences of nutrient availability between thaw gradient experiment and nutrient addition experiment, we compared leaf N and P concentrations as well as inorganic N and P concentrations in soil extracts between the two experiments. We found that the ranges of nutrient availability in the fertilization experiment were comparable to the variations observed in the thaw gradient experiment (Figure 2; Table S2). Specifically, both leaf N concentration and soil inorganic N concentration at the early thaw stage were 1.1 and 1.4 times higher than those at the control. Accordingly, N addition increased them 1.1 and 1.3 times. Analogously, both leaf P concentration and soil inorganic P concentration were highest at the later thaw stage about 1.6 mg g<sup>-1</sup> and 2.6 mg kg<sup>-1</sup>, respectively, which were similar to the corresponding values under P addition treatment (1.6 mg g<sup>-1</sup> and 3.0 mg kg<sup>-1</sup>, respectively). These comparisons suggested that the range of nutrient availability was comparable between the thaw gradient experiment and the fertilization experiment. Such a pattern might be due to the considerable nutrient losses through ammonia volatilization as well as nitrate and phosphate leaching after fertilizer additions (Norberg & Aronsson, 2020), resulting in the less nutrient residue in soil. Overall, it is acceptable to combine the two experiments to explore the potential role of soil nutrient availability in regulating ecosystem C dynamics upon permafrost thaw.

#### 2.5 | Statistical analyses

All experimental data were checked for normal distributions with the Shapiro–Wilk test and then analyzed by the following three steps. First, to explore the effects of permafrost collapse (or N and P treatments) on ecosystem C fluxes, we conducted repeated-measures analyses of variance (ANOVA) with sampling date as the within-subject effect and thaw stage (or N and P treatments) as between-subject effect. Meanwhile, one-way ANOVAs were carried out to investigate the differences of all the abiotic (soil temperature and moisture, pH, clay content, and soil N and P availability) and biotic factors (leaf N and P concentrations, LAI, the relative abundance of forb, soil and root surface acid phosphatase) among various thaw stages (or N and P treatments). Tukey's HSD for multiple comparisons was used to evaluate differences for the abiotic and biotic factors along the thaw sequence at a significance level of  $\alpha = 0.05$ .

Second, we performed regression analyses to explore the relationships of ecosystem C fluxes with biotic (LAI, leaf N and P concentrations, and the relative abundance of forb) and abiotic factors (soil temperature, moisture, and N and P availability) along the thaw sequence. To match those measurements about biotic and abiotic factors, only the  $\rm CO_2$  fluxes determined in 2018 were used during the corresponding analyses. Considering the close associations among inorganic N/P concentrations in soil extracts and solution and soil N/P mineralization rate, we created a comprehensive index using the

first component of principal component analysis (PCA) to represent soil N/P availability (Table S3). Given that soil P availability played an important role in regulating ecosystem  $CO_2$  fluxes along the thaw sequence, we also explored the potential drivers of soil P availability by examining its relationships with the corresponding explanatory variables (soil temperature, moisture, pH, clay content, metal minerals, soil and root surface acid phosphatase). All the above-mentioned statistics were conducted with SPSS 20.0 (IBM SPSS).

Third, we constructed two structural equation models (SEMs) to explore the causal and interactive pathways regulating ecosystem  ${\rm CO}_2$  fluxes along the thaw sequence. Base models were established on the basis of prior knowledge about the possible effects of explanatory variables on GPP and NEP. The model fitness was evaluated using the  $\chi^2$  test and root mean squared error approximation (RMSEA) (Grace, 2006). SEM analyses were conducted using AMOS 21.0 (Amos Development Corporation).

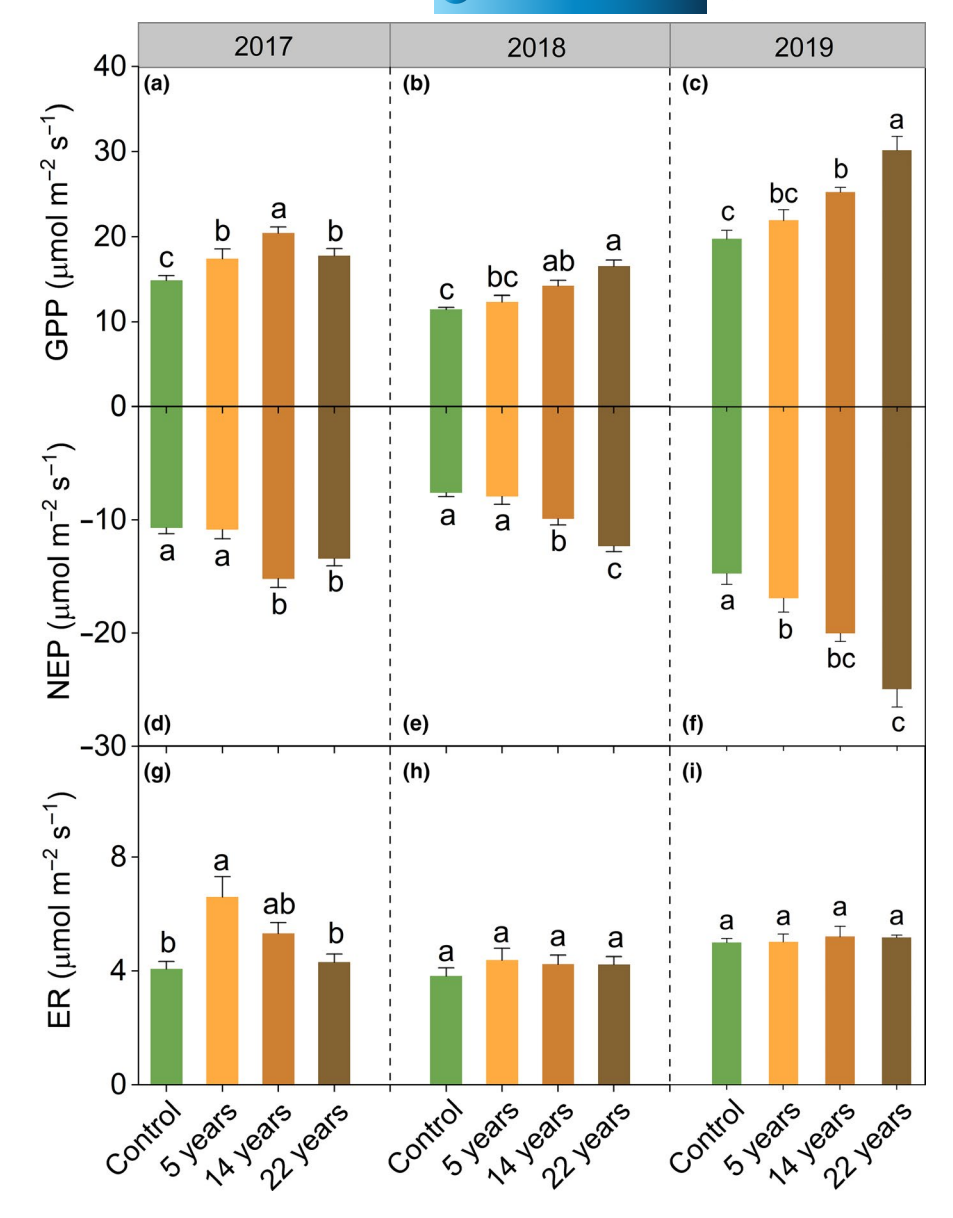
#### 3 | RESULTS

# 3.1 | Changes in ecosystem C fluxes and the associated drivers along the thaw sequence

GPP, NEP, and ER exhibited significant differences among various thaw stages (Figure 1; Table S4). Along the thaw sequence, seasonal mean GPP initially increased and subsequently declined in 2017  $(F_{3.36} = 9.9, p < 0.001;$  Figure 1a), but progressively increased in 2018  $(F_{3.36} = 13.6, p < 0.001; Figure 1b)$  and 2019  $(F_{3,36} = 18.2, p < 0.001; Figure 1b)$ Figure 1c). Accordingly, seasonal mean NEP initially declined and subsequently increased with the lowest in the middle thaw stage in 2017 ( $F_{3.36} = 7.1$ , p < 0.001; Figure 1d), yet exhibited a decreasing trend along the thaw gradient in 2018 ( $F_{3,36} = 20.4$ , p < 0.001; Figure 1e) and 2019 ( $F_{3,36} = 18.4$ , p < 0.001; Figure 1f). However, compared with the uncollapsed area, the seasonal mean ER did not show significant changes along the thaw sequence, except for a significant increase (4.2  $\pm$  0.8 [mean  $\pm$  SD] vs. 6.6  $\pm$  2.4  $\mu$ mol m<sup>-2</sup> s<sup>-1</sup>;  $F_{3.36} = 7.1$ , p < 0.001) at the initial thaw stage in 2017 (Figure 1g-i). These results indicated that the changes in ecosystem C sequestration along the thaw sequence were mainly determined by GPP. Notably, the differences in the observed patterns of GPP and NEP among three experimental years were largely due to the heavy rain disturbance in 2017, which strongly disturbed plants at the late thaw stage. Although this phenomenon induced by the extreme precipitation event only occurred once since 2014 in our study site (Figure S2), the effects of heavy rain on plant growth could have serious consequences for ecosystem C cycling (Figure S3).

Similar to ecosystem C fluxes, the associated drivers also displayed large variations along the thaw sequence (Figure 2). Permafrost thaw altered leaf N and P concentrations as well as soil N and P availability. Concisely, leaf N concentration initially increased from 24.6  $\pm$  1.6 mg g<sup>-1</sup> in the uncollapsed area to 27.4  $\pm$  1.4 mg g<sup>-1</sup> at the early stage, but subsequently decreased to 23.8  $\pm$  1.0 mg g<sup>-1</sup> at the late thaw stage ( $F_{3.36} = 17.6$ , p < 0.001; Figure 2a). Similarly,

FIGURE 1 Changes in gross primary productivity (GPP; a, b, c), net ecosystem productivity (NEP; d, e, f), ecosystem respiration (ER; g, h, i) along the thaw sequence in 2017, 2018, and 2019. GPP, NEP, and ER are averaged across the growing season for each thaw stage in three experimental years. Negative NEP indicates ecosystem C uptake. Different colors correspond to the collapse time prior to 2017, and different letters represent significant differences along the thaw sequence (Tukey's HSD test, p < 0.05). Error bars denote standard errors (n = 10) [Colour figure can be viewed at wileyonlinelibrary.com



inorganic N concentrations in both soil extracts and solution and soil N mineralization rate were 1.4, 6.1, and 2.0 times greater at the early thaw stage compared with the control, but subsequently decreased along the thaw sequence and approached their minimum at the late thaw stage  $(40.6 \pm 14.1 \text{ mg kg}^{-1}, 0.16 \pm 0.04 \text{ mg L}^{-1},$ and 200.0  $\pm$  106.8 ng cm<sup>-2</sup> day<sup>-1</sup>, respectively; Figure 2c,e,g). By contrast, leaf P concentration ( $F_{3,36} = 16.2$ , p < 0.001; Figure 2b), soil inorganic P concentrations in both soil extracts ( $F_{3.36} = 27.3$ , p < 0.001; Figure 2d) and solution ( $F_{3,36} = 12.4, p < 0.001$ ; Figure 2f) and soil P mineralization rate ( $F_{3,36} = 21.5$ , p < 0.001; Figure 2h) progressively increased with thaw time, respectively. In addition, soil temperature ( $F_{3,36} = 3.5$ , p < 0.05) and moisture ( $F_{3,36} = 25.9$ , p < 0.001) decreased immediately after permafrost thaw, but increased thereafter close to the corresponding values under the control. Likewise, LAI ( $F_{3.36} = 6.5$ , p < 0.001) and the relative abundance of forb ( $F_{3,36} = 7.5$ , p < 0.001) progressively increased with time since permafrost collapse (Table S5).

# 3.2 | Linking thaw-induced changes in ecosystem C fluxes to biotic and abiotic factors

GPP did not show any significant relationships with soil temperature ( $F_{1,38}=1.1,\,R^2=0.03,\,p=0.29$ ; Figure 3a), or leaf N concentration ( $F_{1,38}=1.1,\,R^2=0.03,\,p=0.29$ ; Figure 3f), but increased with soil moisture ( $F_{1,38}=5.1,\,R^2=0.12,\,p<0.05$ ; Figure 3b), LAI ( $F_{1,38}=79.0,\,R^2=0.68,\,p<0.001$ ; Figure 3e), leaf P concentration ( $F_{1,38}=21.2,\,R^2=0.35,\,p<0.001$ ; Figure 3g), and the relative abundance of forb ( $F_{1,38}=11.1,\,R^2=0.23,\,p<0.01$ ; Figure 3h). Moreover, variations in GPP along the thaw sequence did not have significant linkage with soil N availability ( $F_{1,38}=3.6,\,R^2=0.03,\,p=0.25$ ; Figure 3c), but were positively associated with soil P availability ( $F_{1,38}=32.3,\,R^2=0.46,\,p<0.001$ ; Figure 3d). SEM analysis revealed that the combination of these direct and indirect effects accounted for 79% of the variance in GPP (Figure 4a). It was directly regulated by the relative abundance of forb, LAI, and leaf P concentration, and indirectly

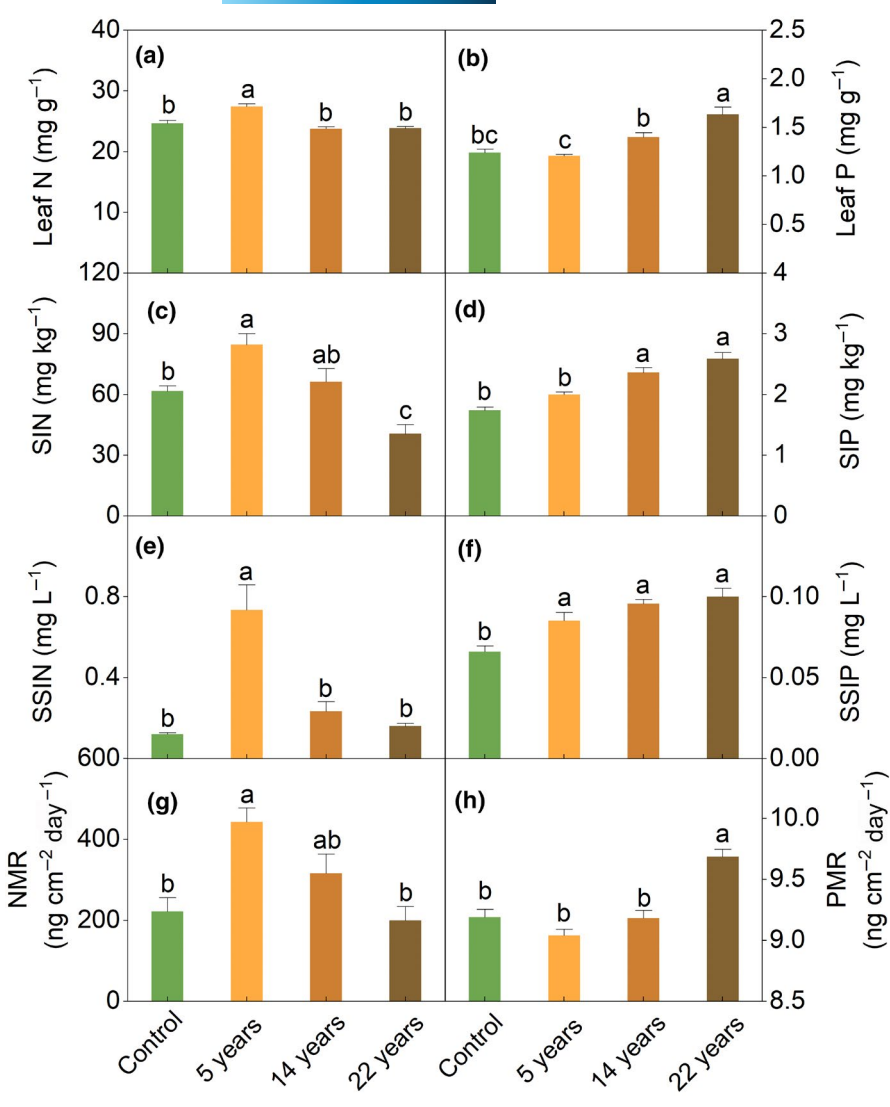


FIGURE 2 Changes in leaf nitrogen (N) and phosphorus (P) concentrations (a, b), inorganic N and P concentrations in soil extracts (SIN, c; SIP, d), inorganic N and P concentrations in soil solution (SSIN, e; SSIP, f) and soil N (NMR, g) and P (PMR, h) mineralization rates along the thaw sequence. Different colors correspond to the collapse time prior to 2017, and different letters represent significant differences along the thaw sequence (Tukey's HSD test, p < 0.05). Error bars denote standard errors (n = 10) [Colour figure can be viewed at wileyonlinelibrary. com]

modulated by soil moisture and P availability. Among these factors, soil P availability was an important driver of ecosystem C fluxes along the thaw sequence (Figure 4b). It had an indirect effect on GPP by improving the relative abundance of forb and leaf P concentration that exerted direct positive effects on GPP or indirect positive effects via elevating LAI (Figure 4a). Likewise, of the abiotic variables, soil P availability had the greatest prediction power for NEP dynamics along the thaw sequence (see Text S3 for details).

The fertilization experiment confirmed the phenomenon observed along the thaw sequence (Figure 5). Specifically, N addition increased soil N availability ( $F_{1,6}=16.7,\,p<0.01$ ) and leaf N content ( $F_{1,6}=8.2,\,p<0.01$ ), reduced leaf P content ( $F_{1,6}=19.4,\,p<0.01$ ), but had no significant effect on soil P availability ( $F_{1,6}=16.7,\,p=0.36$ ). On the contrary, P addition did not alter soil N availability ( $F_{1,6}=5.4,\,p=0.06$ ) and leaf N content ( $F_{1,6}=0,\,p=0.98$ ), but elevated soil P availability ( $F_{1,6}=137.3,\,p<0.001$ ) and leaf P content ( $F_{1,6}=50.7,\,p<0.001$ ; Table S2). Similarly, N and P additions exerted different effects on ecosystem C fluxes,

NDVI, and AGB (Figure 5; Table S2). N addition did not exert any significant effects on GPP ( $F_{1.6} = 1.8, p = 0.23$ ), NEP ( $F_{1.6} = 0.9$ , p = 0.37), NDVI ( $F_{1.6} = 1.9$ , p = 0.22), or AGB ( $F_{1.6} = 1.0$ , p = 0.36), but stimulated ER ( $F_{1.6} = 9.9$ , p < 0.05; see Text S4 for the detailed discussion). By contrast, P addition significantly increased GPP ( $F_{1,6} = 14.0, p < 0.01$ ), NDVI ( $F_{1,6} = 8.2, p < 0.05$ ), and AGB  $(F_{1.6} = 7.2, p < 0.05)$ , but reduced NEP  $(F_{1.6} = 15.4, p < 0.01)$  and had no significant effect on ER ( $F_{1.6} = 3.6$ , p = 0.11). Further regression analyses showed that GPP increased with soil inorganic P concentrations under P addition ( $F_{1.7} = 14.7, p < 0.01$ ; Figure S4d), but did not exhibit any significant relationships with soil inorganic N concentration ( $F_{1,7} = 2.5, p = 0.17$ ; Figure S4a) and inorganic P concentration ( $F_{1.7} = 2.3$ , p = 0.18; Fig. S4b) under N addition, or soil inorganic N concentration under P addition ( $F_{1.7} = 4.2$ , p = 0.09; Figure S4c). Notably, to match permafrost thaw gradient study, we only showed GPP data from the fertilization experiment in the main text. The corresponding NEP and ER results could be found in Supplementary Information (Table S2).

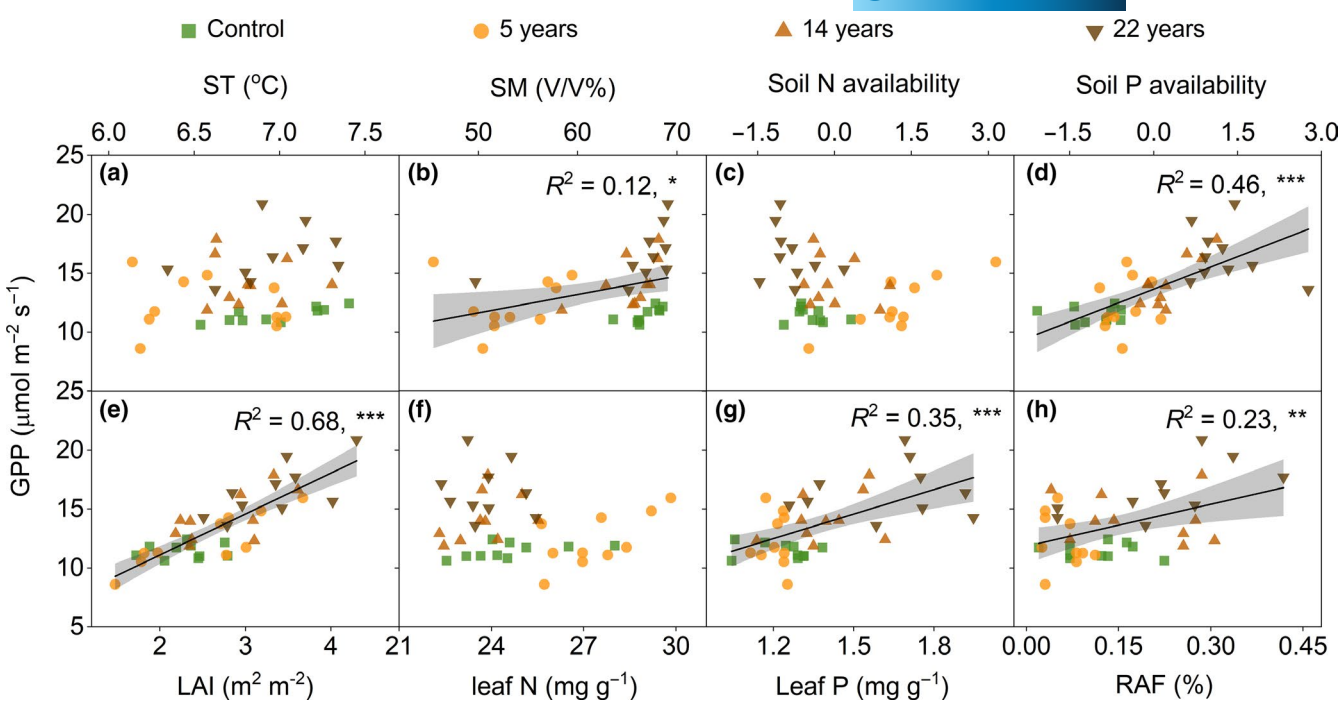


FIGURE 3 Relationships between gross primary productivity (GPP) and soil temperature (ST, a), soil moisture (SM, b), soil nitrogen (N) and phosphorus (P) availability (c, d), leaf area index (LAI, e), leaf N and P concentrations (f, g), and the relative abundance of forb (RAF, h). Soil N/P availability was the first component of principal component analysis (PCA) conducted with inorganic N/P concentrations in soil extracts and solution and soil N/P mineralization rate. The black lines and shades represent the regression lines with 95% confidence intervals. Statistics ( $R^2$  and  $R^2$  values) are shown for the linear regression (\* $R^2$  0.05, \*\* $R^2$  0.001) [Colour figure can be viewed at wileyonlinelibrary.com]

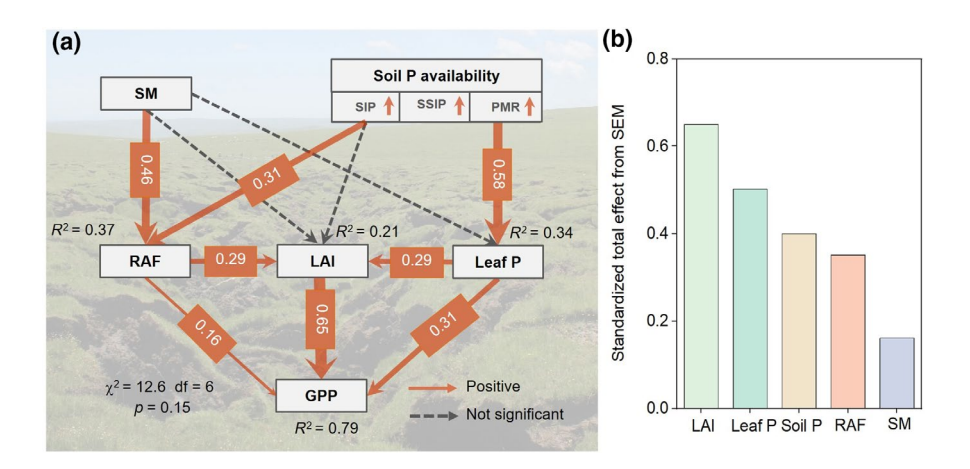


FIGURE 4 Results of structural equation model (SEM) analysis examining the pathways regulating variations in gross primary productivity (GPP, a) along the thaw gradient and standardized total effects on GPP derived from SEM (b). SM, soil moisture indicated by volumetric water content; SIP, soil inorganic phosphorus (P); SSIP, soil solution inorganic P; PMR, soil P mineralization rate; RAF, the relative abundance of forb; LAI, leaf area index; and double-layer rectangle represents the first component from the principal component analysis (PCA) conducted with inorganic P concentrations in soil extracts and soil solution and soil P mineralization rate. The orange or blue arrows indicate positive or negative relationship between variables, respectively. Goodness-of-fit statistics for the models are shown below the model [Colour figure can be viewed at wileyonlinelibrary.com]

# 3.3 | Drivers of soil P availability along the thaw sequence

Permafrost thaw exerted significant effects on the variables associated with soil P availability (Table S5). Specifically, clay content in the surface soil was highest in the uncollapsed area, and progressively

decreased along the thaw gradient ( $F_{3,36}=17.0,\,p<0.001$ ). Soil pH was slightly acidic in our study site, with the maximum at the late thaw stage ( $F_{3,36}=9.4,\,p<0.001$ ). Fe<sub>d</sub> ( $F_{3,36}=1.9,\,p<0.05$ ) and Fe<sub>o</sub> + Al<sub>o</sub> ( $F_{3,36}=5.1,\,p<0.01$ ) initially increased and subsequently declined, whereas Fe<sub>p</sub> + Al<sub>p</sub> showed exhibited no significant difference along the thaw sequence ( $F_{3,36}=0.9,\,p=0.43$ ). Both soil

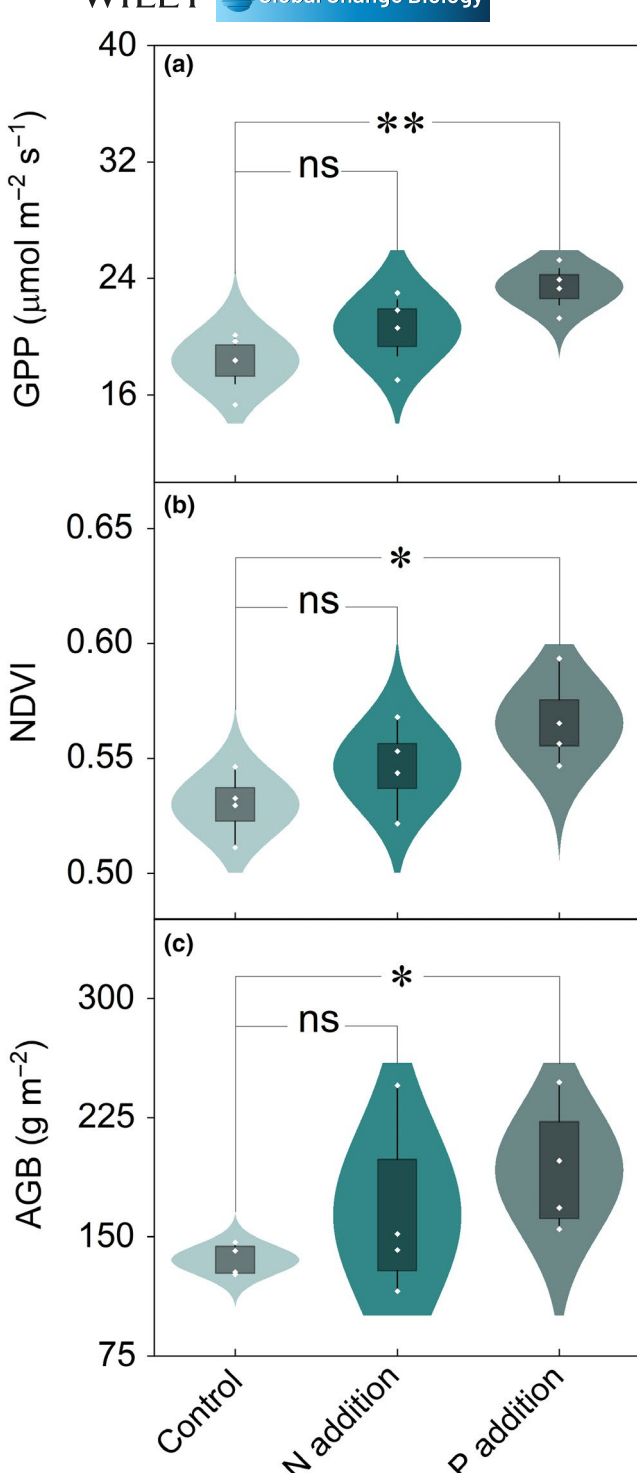


FIGURE 5 Effects of nitrogen (N) and phosphorus (P) additions on gross primary productivity (GPP, a), the normalized difference vegetation index (NDVI, b) and aboveground biomass (AGB, c). The white circles in the boxes indicate actual measured value (n=4). Asterisk (\*) represents the significant difference between control and nutrient treatment (\*p < 0.05, \*\* p < 0.01); ns, insignificant difference [Colour figure can be viewed at wileyonlinelibrary.com]

( $F_{3,36} = 4.2$ , p < 0.05) and root surface acid phosphatase ( $F_{3,36} = 6.2$ , p < 0.01) were lowest at the late thaw stage. Of all variables

examined (Figure 6), soil P availability was positively related to soil pH ( $F_{1,38}=13.8$ ,  $R^2=0.27$ , p<0.01), but negatively associated with clay content ( $F_{1,38}=30.5$ ,  $R^2=0.45$ , p<0.001). However, soil P availability was not significantly associated with soil temperature ( $F_{1,38}=0.1$ ,  $R^2=0.00$ , p=0.73), soil moisture ( $F_{1,38}=2.1$ ,  $R^2=0.03$ , p=0.16), or Fe/Al minerals (Fe<sub>d</sub>:  $F_{1,38}=3.3$ ,  $R^2=0.08$ , p=0.08 and Fe<sub>o</sub> + Al<sub>o</sub>:  $F_{1,38}=0.9$ ,  $R^2=0.02$ , P=0.34).

### 4 | DISCUSSION

Based on the combination of systematic observations along the thaw sequence and additional isotopic labeling and fertilization experiments, this study examined the potential role of soil nutrient availability in regulating ecosystem C fluxes after permafrost thaw. Our results indicated that along the thaw sequence, soil N availability exhibited an initial increase but a subsequent decrease, whereas soil P availability progressively increased. Our results also revealed that changes in ecosystem C uptake along the thaw sequence were mainly driven by GPP and there was a significant positive linkage between GPP and soil P availability, but not between GPP and soil N availability. The fertilization experiment confirmed that plant growth was more sensitive to P addition than N addition. These findings highlight that soil P availability, which has not attracted too much attention by the permafrost C research community, plays a key role in regulating ecosystem C dynamics upon permafrost thaw.

The close association between GPP and soil P availability observed in this study could be attributed to the following two aspects. First, soil P availability could regulate GPP by relieving P limitation. In P-limited ecosystems, the increased soil P availability can enhance leaf P concentration (Tessier & Raynal, 2003), which could provide benefits for a series of physiological processes including the synthesis of nucleotides, enzymes, and metabolisms since leaf P is an indispensable component of plant cell compounds (Taiz & Zeiger, 2006). Consequently, the increased leaf P concentration could promote plant growth by stimulating enzyme activity associated with photosynthesis and improving light-use efficiency (Lombardozzi et al., 2018). The increased leaf P concentration could also induce larger LAI, and then enhance vegetation growth by intercepting more light resources (Li, Peng, Zhang, et al., 2019; Street et al., 2018). Second, soil P availability could regulate GPP by altering vegetation composition. In support of this argument, our results showed that increases in soil P availability elevated the relative abundance of forb, and then caused an increase in vegetation community diversity (Figure S5). Given that higher community diversity is generally associated with stronger interspecific complementarity and higher resource utilization efficiency (García-Palacios et al., 2018; Gross et al., 2007), the increased soil P availability could thus stimulate GPP by promoting community diversity. Additionally, the increased relative abundance of forb also resulted in larger leaf area (i.e., LAI, Table S5), which could intercept more light resources so as to enhance GPP (Li, Peng, Zhang, et al., 2019; Street et al., 2018).

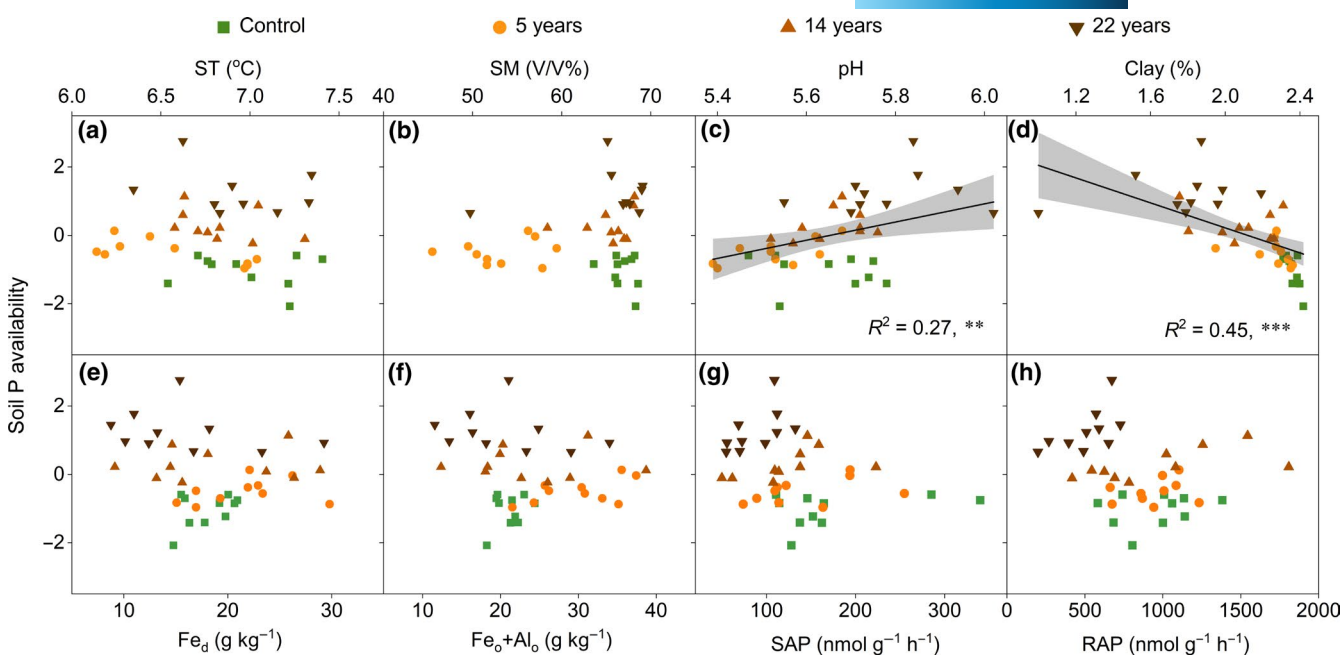


FIGURE 6 Relationships of soil phosphorus (P) availability with soil temperature (ST, a), soil moisture (SM, b), soil pH (c), clay content (d), free Fe -(hydr) oxides (Fe<sub>d</sub>, e), amorphous Fe/Al-(hydr) oxides (Fe<sub>o</sub> + Al<sub>o</sub>, f), soil (SAP, g) and root surface acid phosphatase activity (RAP, h). Soil P availability was the first component of principal component analysis (PCA) conducted with inorganic P concentrations in soil extracts and soil solution and soil P mineralization rate. The black lines and shades represent the regression lines with 95% confidence intervals. Statistics ( $R^2$  and P value) are shown for the linear regression (\*\*P < 0.01, \*\*\*P < 0.001) [Colour figure can be viewed at wileyonlinelibrary. com]

An interesting question arises about what causes the increase in soil P availability after permafrost thaw. This pattern could be explained by the following non-exclusive mechanisms. First, increased plant-available P may come from the desorption of the soil inorganic P from mineral particles. In acidic soils, large amounts of inorganic P are often adsorbed on the surface of clay minerals and metal oxides by forming various complexes owing to their large specific surface areas and adsorption sites, which render them unavailable to plants (Arai & Sparks, 2007). However, permafrost collapse, particularly the formation of thermo-erosion gully exerted significant effects on soil mineral content, especially clay content (Table S5). It has been reported that decreasing soil mineral content can be expected to result in the desorption of inorganic P (Devau et al., 2010), which may be thus beneficial to transfer the absorbed inorganic P to plant-available inorganic P (Table S6). Second, the increased plant-available P may be derived from soil organic P mineralization. Organic P mainly exists in stabilized forms in soil, which can be unable to directly absorbed by plant. It is widely accepted that organic P can be mineralized to plant-available through phosphatase secreted by soil organisms and plant roots, and these processes are also highly dependent on soil mineral content and soil pH (Turner et al., 2007). Decreasing mineral content can be beneficial to diminish its protective effects on soil organic P (Table S6), and increasing pH can be expected to improve phosphatase activities in acidic soils (Shen et al., 2011). In our study, though soil P availability was not significantly associated with soil and root surface acid phosphatase, the decreased soil clay content and increased

soil pH may lead to the higher organic P mineralization rate and soil P availability (Figure 6).

It has been reported that permafrost thaw may promote plant growth by increasing soil N availability (Finger et al., 2016; Hewitt et al., 2020; Keuper et al., 2017; Salmon et al., 2016). In contrast to this prevailing view, we did not detect a significant relationship between GPP and soil N availability along the thaw sequence, which does not support part of our initial hypothesis that permafrost thaw could promote plant growth and enhance ecosystem C uptake by improving soil N status. This phenomenon could be due to the fact that soil P availability is the most limiting factor for plant growth relative to soil N availability in this study site. According to Liebig's Law of the Minimum, plant growth is controlled by the most limiting nutrient and not by the plentiful nutrients (Liebig, 1842). Thus, we did not observe an apparent association between GPP and soil N availability in this permafrost ecosystem.

In summary, using 3-year field observations along the thaw sequence, combined with an in-situ fertilization experiment, this study demonstrated that permafrost thaw stimulated ecosystem C uptake by increasing soil P availability. This finding has two important implications for predicting permafrost C dynamics. First, permafrost thaw could promote plant growth and enhance ecosystem C uptake in permafrost regions, which is supported by previous reports obtained from the Arctic and Boreal regions (McGuire et al., 2009; Natali et al., 2012). The consistent observations derived from highaltitude and high-latitude permafrost areas suggest that permafrost thaw-induced C losses may be partly mitigated by the increased

plant productivity, which may, in turn, weaken the strength of permafrost C-climate feedback. Second, the positive association between GPP and soil P availability observed in this study suggests that soil P status might be another key factor regulating plant productivity in permafrost regions, and provides a novel perspective into C-nutrient interactions after permafrost thaw. Therefore, the dynamics of soil P availability should be considered when predicting the trajectory of permafrost C dynamics under continuous climate warming. Nevertheless, a greater number of thermo-erosion gullies, more years of observation and more levels of nutrient addition are needed to further improve our understanding on this issue in the future.

#### **ACKNOWLEDGEMENTS**

We thank two anonymous reviewers who have provided constructive comments to improve this manuscript. This work was supported by the National Natural Science Foundation of China (31825006, 31988102, and 91837312), the Second Tibetan Plateau Scientific Expedition and Research (STEP) program (2019QZKK0106), Key Research Program of Frontier Sciences, Chinese Academy of Sciences (QYZDB-SSW-SMC049), and China National Postdoctoral Program for Innovative Talents (BX20200363).

#### **CONFLICT OF INTEREST**

The authors declare that they have no conflict of interest.

### DATA AVAILABILITY STATEMENT

The data that support the findings of this study are available from the corresponding author upon reasonable request.

### ORCID

Benjamin W. Abbott https://orcid.org/0000-0001-5861-3481
Yuanhe Yang https://orcid.org/0000-0002-5399-4606

## REFERENCES

- Arai, Y., & Sparks, D. L. (2007). Phosphate reaction dynamics in soils and soil components: A multiscale approach. *Advances in Agronomy*, 94(06), 135–179. https://doi.org/10.1016/S0065-2113(06)94003-6
- Bray, R. H., & Kurtz, L. T. (1945). Determination of total, organic, and available forms of phosphorus in soils. *Soil Science*, *59*(1), 39–46. https://doi.org/10.1097/00010694-194501000-00006
- Brown, J., & Romanovsky, V. E. (2008). Report from the International Permafrost Association: State of permafrost in the first decade of the 21st century. *Permafrost and Periglacial Processes*, 19(2), 255–260. https://doi.org/10.1002/ppp.618
- Chadburn, S. E., Burke, E. J., Cox, P. M., Friedlingstein, P., Hugelius, G., & Westermann, S. (2017). An observation-based constraint on permafrost loss as a function of global warming. *Nature Climate Change*, 7(5), 340–344. https://doi.org/10.1038/nclimate3262
- Chapin, F. S., Shaver, G. R., Giblin, A. E., Nadelhoffer, K. J., & Laundre, J. A. (1995). Responses of arctic tundra to experimental and observed changes in climate. *Ecology*, 76(3), 694–711. https://doi. org/10.2307/1939337
- Chen, L., Liang, J., Qin, S., Liu, L., Fang, K., Xu, Y., Ding, J., Li, F., Luo, Y., & Yang, Y. (2016). Determinants of carbon release from the active

- layer and permafrost deposits on the Tibetan Plateau. Nature Communications, 7, 13046. https://doi.org/10.1038/ncomms13046
- Christiansen, C. T., Lafreniere, M. J., Henry, G. H. R., & Grogan, P. (2018). Long-term deepened snow promotes tundra evergreen shrub growth and summertime ecosystem net CO<sub>2</sub> gain but reduces soil carbon and nutrient pools. *Global Change Biology*, 24(8), 3508–3525. https://doi.org/10.1111/gcb.14084
- Commane, R., Lindaas, J., Benmergui, J., Luus, K. A., Chang, R. Y.-W., Daube, B. C., Euskirchen, E. S., Henderson, J. M., Karion, A., Miller, J. B., Miller, S. M., Parazoo, N. C., Randerson, J. T., Sweeney, C., Tans, P., Thoning, K., Veraverbeke, S., Miller, C. E., & Wofsy, S. C. (2017). Carbon dioxide sources from Alaska driven by increasing early winter respiration from Arctic tundra. *Proceedings of the National Academy of Sciences of the United States of America*, 114(21), 5361–5366. https://doi.org/10.1073/pnas.1618567114
- Deng, M., Liu, L., Sun, Z., Piao, S., Ma, Y., Chen, Y., Wang, J., Qiao, C., Wang, X., & Li, P. (2016). Increased phosphate uptake but not resorption alleviates phosphorus deficiency induced by nitrogen deposition in temperate *Larix principis-rupprechtii* plantations. *New Phytologist*, 212(4), 1019–1029. https://doi.org/10.1111/nph.14083
- Devau, N., Cadre, E. L., Hinsinger, P., & Gérard, F. (2010). A mechanistic model for understanding root-induced chemical changes controlling phosphorus availability. *Annals of Botany*, 105, 1183–1197. https://doi.org/10.1093/aob/mcq098
- Ding, J., Li, F., Yang, G., Chen, L., Zhang, B., Liu, L., Fang, K., Qin, S., Chen, Y., Peng, Y., Ji, C., He, H., Smith, P., & Yang, Y. (2016). The permafrost carbon inventory on the Tibetan Plateau: A new evaluation using deep sediment cores. *Global Change Biology*, 22(8), 2688–2701. https://doi.org/10.1111/gcb.13257
- Edwards, P. J., Frauke, F. D., & Kaiser-Bunbury, C. N. (2015). The nutrient economy of *Lodoicea maldivica*, a monodominant palm producing the world's largest seed. *New Phytologist*, 206(3), 990–999. https://doi.org/10.1111/nph.13272
- Finger, R. A., Turetsky, M. R., Kielland, K., Ruess, R. W., Mack, M. C., & Euskirchen, E. S. (2016). Effects of permafrost thaw on nitrogen availability and plant-soil interactions in a boreal Alaskan lowland. *Journal of Ecology*, 104(6), 1542–1554. https://doi.org/10.1111/1365-2745.12639
- García-Palacios, P., Gross, N., Gaitán, J., & Maestre, F. T. (2018). Climate mediates the biodiversity-ecosystem stability relationship globally. Proceedings of the National Academy of Sciences of the United States of America, 115(3), 8400-8405. https://doi.org/10.1073/ pnas.1800425115
- Grace, J. (2006). Structural equation modeling and natural systems.

  Academic Press.
- Gross, N., Suding, K. N., Lavorel, S., & Roumet, C. (2007). Complementarity as a mechanism of coexistence between functional groups of grasses. *Journal of Ecology*, 95(6), 1296–1305. https://doi.org/10.1111/j.1365-2745.2007.01303.x
- Hewitt, R. E., Devan, M. R., Lagutina, I. V., Genet, H., Mcguire, A. D., Taylor, D. L., & Mack, M. C. (2020). Mycobiont contribution to tundra plant acquisition of permafrost-derived nitrogen. New Phycologist, 226(1), 126–141. https://doi.org/10.1111/nph.16235
- Hou, E., Luo, Y., Kuang, Y., Chen, C., Lu, X., Jiang, L., Luo, X., & Wen, D. (2020). Global meta-analysis shows pervasive phosphorus limitation of aboveground plant production in natural terrestrial ecosystems. *Nature Communications*, 11, 637. https://doi.org/10.1038/s41467-020-14492-w
- Hugelius, G., Strauss, J., Zubrzycki, S., Harden, J. W., Schuur, E. A. G., Ping, C.-L., Schirrmeister, L., Grosse, G., Michaelson, G. J., Koven, C. D., O'Donnell, J. A., Elberling, B., Mishra, U., Camill, P., Yu, Z., Palmtag, J., & Kuhry, P. (2014). Estimated stocks of circumpolar permafrost carbon with quantified uncertainty ranges and identified data gaps. *Biogeosciences*, 11(23), 6573–6593. https://doi. org/10.5194/bg-11-6573-2014

- Jin, H., Luo, D., Wang, S., Lü, L., & Wu, J. (2011). Spatiotemporal variability of permafrost degradation on the Qinghai-Tibet Plateau. Sciences in Cold and Arid Regions, 3(4), 0281-0305. https://doi.org/10.3724/SP.J.1226.2011.00281
- Keiluweit, M., Bougoure, J. J., Nico, P. S., Pett-Ridge, J., Weber, P. K., & Kleber, M. (2015). Mineral protection of soil carbon counteracted by root exudates. *Nature Climate Change*, 5(6), 588–595. https://doi. org/10.1038/nclimate2580
- Keuper, F., Dorrepaal, E., van Bodegom, P. M., Van, L. R., Venhuizen, G., Hal, J. V., & Aerts, R. (2017). Experimentally increased nutrient availability at the permafrost thaw front selectively enhances biomass production of deep-rooting subarctic peatland species. *Global Change Biology*, 23(10), 4257–4266. https://doi.org/10.1111/gcb.13804
- Kicklighter, D. W., Melillo, J. M., Monier, E., Sokolov, A. P., & Zhuang, Q. (2019). Future nitrogen availability and its effect on carbon sequestration in Northern Eurasia. *Nature Communications*, 10, 3024. https://doi.org/10.1038/s41467-019-10944-0
- Kokelj, S., & Jorgenson, M. T. (2013). Advances in thermokarst research. Permafrost and Periglacial Processes, 24(2), 108–119. https://doi. org/10.1002/ppp.1779
- Lalonde, K., Mucci, A., Ouellet, A., & Gélinas, Y. (2012). Preservation of organic matter in sediments promoted by iron. *Nature*, 483(7388), 198–200. https://doi.org/10.1038/nature10855
- Li, F., Peng, Y., Chen, L., Yang, G., Abbott, B. W., Zhang, D., Fang, K., Wang, G., Wang, J., Yu, J., Liu, L., Zhang, Q., Chen, K., Mohammat, A., & Yang, Y. (2019). Warming alters surface soil organic matter composition despite unchanged carbon stocks in a Tibetan permafrost ecosystem. Functional Ecology, 34(4), 911–922. https://doi. org/10.1111/1365-2435.13489
- Li, F., Peng, Y., Natali, S. M., Chen, K., Han, T., Yang, G., Ding, J., Zhang, D., Wang, G., Wang, J., Yu, J., Liu, F., & Yang, Y. (2017). Warming effects on permafrost ecosystem carbon fluxes associated with plant nutrients. *Ecology*, 98(11), 2851–2859. https://doi. org/10.1002/ecy.1975
- Li, F., Peng, Y., Zhang, D., Yang, G., Fang, K., Wang, G., Wang, J., Yu, J., Zhou, G., & Yang, Y. (2019). Leaf area rather than photosynthetic rate determines the response of ecosystem productivity to experimental warming in an alpine steppe. *Journal of Geophysical Research: Biogeosciences*, 124(7), 2277–2287. https://doi.org/10.1029/2019J G005193
- Liebig, J. (1842). Animal chemistry, or organic chemistry in its application to physiology and pathology. Johnson Reprint Corporation.
- Liu, F., Chen, L., Abbott, B. W., Xu, Y., Yang, G., Kou, D., Qin, S., Strauss, J., Wang, Y., Zhang, B., & Yang, Y. (2018). Reduced quantity and quality of SOM along a thaw sequence on the Tibetan Plateau. Environmental Research Letters, 13, 104017. https://doi. org/10.1088/1748-9326/aae43b
- Lombardozzi, D. L., Smith, N. G., Cheng, S. J., Dukes, J. S., Sharkey, T. D., Rogers, A., Fisher, R., & Bonan, G. B. (2018). Triose phosphate limitation in photosynthesis models reduces leaf photosynthesis and global terrestrial carbon storage. *Environmental Research Letters*, 13, 074025. https://doi.org/10.1088/1748-9326/aacf68
- Mao, C., Kou, D., Chen, L., Qin, S., Zhang, D., Peng, Y., & Yang, Y. (2020). Permafrost nitrogen status and its determinants on the Tibetan Plateau. *Global Change Biology*, *26*(9), 5290–5302. https://doi.org/10.1111/gcb.15205
- Marx, M. C., Wood, M., & Jarvis, S. C. (2001). A microplate fluorimetric assay for the study of enzyme diversity in soils. *Soil Biology and Biochemistry*, 33(12–13), 1633–1640. https://doi.org/10.1016/S0038-0717(01)00079-7
- McGuire, A. D., Anderson, L. G., Christensen, T. R., Dallimore, S., Guo, L., Hayes, D. J., Heimann, M., Lorenson, T. D., Macdonald, R. W., & Roulet, N. (2009). Sensitivity of the carbon cycle in the Arctic to climate change. *Ecological Monographs*, 79(4), 523–555. https://doi.org/10.1890/08-2025.1

- McGuire, A. D., Genet, H., Lyu, Z., Pastick, N., Stackpoole, S., Birdsey, R., D'Amore, D., He, Y., Rupp, T. S., Striegl, R., Wylie, B. K., Zhou, X., Zhuang, Q., & Zhu, Z. (2018). Assessing historical and projected carbon balance of Alaska: A synthesis of results and policy/management implications. *Ecological Applications*, 28(6), 1396–1412. https://doi.org/10.1002/eap.1768
- Meredith, M. P., Sommerkorn, M., Cassotta, S., Derksen, C., & Schuur, E. A. G. (2019). Polar regions In: IPCC special report on the ocean and cryosphere in a changing climate. Cambridge University Press.
- Mishra, U., Hugelius, G., Shelef, E., Yang, Y., Strauss, J., Lupachev, A., Harden, J. W., Jastrow, J. D., Ping, C.-L., Riley, W. J., Schuur, E. A. G., Matamala, R., Siewert, M., Nave, L. E., Koven, C. D., Fuchs, M., Palmtag, J., Kuhry, P., Treat, C. C., ... Orr, A. (2021). Spatial heterogeneity and environmental predictors of permafrost region soil organic carbon stocks. *Science Advances*, 7(9), eaaz5236. https://doi.org/10.1126/sciadv.aaz5236
- Mu, C., Abbott, B. W., Zhao, Q., Su, H., Wang, S., Wu, Q., & Wu, X. (2017). Permafrost collapse shifts alpine tundra to a carbon source but reduces N<sub>2</sub>O and CH<sub>4</sub> release on the northern Qinghai-Tibetan Plateau: Permafrost collapse and greenhouse gases. Geophysical Research Letters, 44(17), 8945–8952. https://doi.org/10.1002/2017GL074338
- Natali, S. M., Schuur, E. A. G., & Rubin, R. L. (2012). Increased plant productivity in Alaskan tundra as a result of experimental warming of soil and permafrost. *Journal of Ecology*, 100(2), 488–498. https://doi.org/10.1111/j.1365-2745.2011.01925.x
- Natali, S. M., Schuur, E. A. G., Webb, E. E., Pries, C. E. H., & Crummer, K. G. (2014). Permafrost degradation stimulates carbon loss from experimentally warmed tundra. *Ecology*, 95(3), 602–608. https://doi.org/10.1890/13-0602.1
- Natali, S. M., Watts, J. D., Rogers, B. M., Potter, S., Ludwig, S. M., Selbmann, A.-K., Sullivan, P. F., Abbott, B. W., Arndt, K. A., Birch, L., Björkman, M. P., Bloom, A. A., Celis, G., Christensen, T. R., Christiansen, C. T., Commane, R., Cooper, E. J., Crill, P., Czimczik, C., ... Zona, D. (2019). Author correction: Large loss of CO<sub>2</sub> in winter observed across the northern permafrost region. *Nature Climate Change*, 9, 852–857. https://doi.org/10.1038/s41558-019-0592-8
- Norberg, L., & Aronsson, H. (2020). Effects of cover crops sown in autumn on N and P leaching. *Soil Use and Management*, 36(2), 200–211. https://doi.org/10.1111/sum.12565
- Parazoo, N. C., Commane, R., Wofsy, S. C., Koven, C. D., & Miller, C. (2016). Detecting regional patterns of changing CO<sub>2</sub> flux in Alaska. Proceedings of the National Academy of Sciences of the United States of America, 113(28), 7733-7738. https://doi.org/10.1073/pnas.1601085113
- Pedersen, E. P., Bo, E., & Michelsen, A. (2020). Foraging deeply: Depth-specific plant nitrogen uptake in response to climate-induced N-release and permafrost thaw in the High Arctic. *Global Change Biology*, 26(11), 6523–6536. https://doi.org/10.1111/gcb.15306
- Peñuelas, J., Poulter, B., Sardans, J., Ciais, P., van der Velde, M., Bopp, L., Boucher, O., Godderis, Y., Hinsinger, P., Llusia, J., Nardin, E., Vicca, S., Obersteiner, M., & Janssens, I. A. (2013). Human-induced nitrogen-phosphorus imbalances alter natural and managed ecosystems across the globe. *Nature Communications*, 4, 2934. https:// doi.org/10.1038/ncomms3934
- Reich, P. B., Oleksyn, J., & Wright, I. J. (2009). Leaf phosphorus influences the photosynthesis-nitrogen relation: A cross-biome analysis of 314 species. *Oecologia*, 160, 207–212. https://doi.org/10.1007/s00442-009-1291-3
- Salmon, V. G., Soucy, P., Mauritz, M., Celis, G., Natali, S. M., Mack, M. C., & Schuur, E. A. G. (2016). Nitrogen availability increases in a tundra ecosystem during five years of experimental permafrost thaw. *Global Change Biology*, 22(5), 1927–1941. https://doi.org/10.1111/ gcb.13204
- Schuur, E. A. G., McGuire, A. D., Schädel, C., Grosse, G., Harden, J. W., Hayes, D. J., Hugelius, G., Koven, C. D., Kuhry, P., Lawrence, D. M., Natali, S.

- M., Olefeldt, D., Romanovsky, V. E., Schaefer, K., Turetsky, M. R., Treat, C. C., & Vonk, J. E. (2015). Climate change and the permafrost carbon feedback. *Nature*, 520, 171–179. https://doi.org/10.1038/nature14338
- Shaver, G. R., & lii, F. S. C. (1991). Production: Biomass relationships and element cycling in contrasting arctic vegetation types. *Ecological Monographs*, 61(1), 1–31. https://doi.org/10.2307/1942997
- Shaver, G. R., Rastetter, E. B., & Williams, M. (2007). Functional convergence in regulation of net CO<sub>2</sub> flux in heterogeneous tundra land-scapes in Alaska and Sweden. *Journal of Ecology*, 95(4), 802–817. https://doi.org/10.1111/j.1365-2745.2007.01259.x
- Shen, J., Yuan, L., Zhang, J., Li, H., Bai, Z., Chen, X., Zhang, W., & Zhang, F. (2011). Phosphorus dynamics: From soil to plant. Plant Physiology, 156(3), 997–1005. https://doi.org/10.1104/pp.111.175232
- Street, L. E., Mielke, N., & Woodin, S. J. (2018). Phosphorus availability determines the response of tundra ecosystem carbon stocks to nitrogen enrichment. *Ecosystems*, *21*, 1155–1167. https://doi.org/10.1007/s10021-017-0209-x
- Taiz, L., & Zeiger, E. (2006). *Plant physiology* (4th ed.). Sinauer Associates
- Tessier, J. T., & Raynal, D. J. (2003). Use of nitrogen to phosphorus ratios in plant tissue as an indicator of nutrient limitation and nitrogen saturation. *Journal of Applied Ecology*, 40(3), 523–534. https://doi.org/10.1046/j.1365-2664.2003.00820.x
- Turetsky, M. R., Abbott, B. W., Jones, M. C., Walter Anthony, K., Olefeldt, D., Schuur, E. A. G., Grosse, G., Kuhry, P., Hugelius, G., Koven, C., Lawrence, D. M., Gibson, C., Sannel, A. B. K., & McGuire, A. D. (2020). Carbon release through abrupt permafrost thaw. *Nature Geoscience*, 13, 138–143. https://doi.org/10.1038/s4156 1-019-0526-0
- Turetsky, M. R., Abbott, B. W., Jones, M. C., Walter Anthony, K., Olefeldt, D., Schuur, E. A. G., Koven, C., McGuire, A. D., Grosse, G., Kuhry, P., Hugelius, G., Lawrence, D. M., Gibson, C., & Sannel, A. B. K. (2019). Permafrost collapse is accelerating carbon release. *Nature*, 569, 32–34. https://doi.org/10.1038/d41586-019-01313-4
- Turner, B. L., Richardson, A. E., Mullaney, E. J., Turner, B. L., Richardson, A. E., & Mullaney, E. J. (2007). Inositol phosphates: Linking agriculture and the environment. Academic Press.
- Vitousek, P. M., Porder, S., Houlton, B. Z., & Chadwick, O. A. (2010). Terrestrial phosphorus limitation: Mechanisms, implications, and nitrogen-phosphorus interactions. *Ecological Applications*, 20(1), 5–15. https://doi.org/10.1890/08-0127.1
- Walter Anthony, K., von Deimling, T. S., Nitze, I., Frolking, S., Emond, A., Daanen, R., Anthony, P., Lindgren, P., Jones, B., & Grosse, G. (2018).

- 21st-century modeled permafrost carbon emissions accelerated by abrupt thaw beneath lakes. *Nature Communications*, *9*, 3262. https://doi.org/10.1038/s41467-018-05738-9
- Wang, B., Bao, Q., Hoskins, B., Wu, G., & Liu, Y. (2008). Tibetan Plateau warming and precipitation changes in East Asia. *Geophysical Research Letters*, 35(14), 63–72. https://doi.org/10.1029/2008G L034330
- Wang, B., & French, H. M. (1995). Permafrost on the Tibet Plateau, China. Quaternary Science Reviews, 14(3), 255–274. https://doi. org/10.1016/0277-3791(95)00006-B
- Wieder, W. R., Cleveland, C. C., Smith, W. K., & Todd-Brown, K. (2015). Future productivity and carbon storage limited by terrestrial nutrient availability. *Nature Geoscience*, 8, 441–444. https://doi.org/10.1038/ngeo2413
- Wu, Q., & Zhang, T. (2008). Recent permafrost warming on the Qinghai-Tibet Plateau. *Journal of Geophysical Research Atmospheres*, 113, D13108. https://doi.org/10.1029/2007JD009539
- Yang, G., Peng, Y., Marushchak, M. E., Chen, Y., Wang, G., Li, F., Zhang, D., Wang, J., Yu, J., Liu, L., Qin, S., Kou, D., & Yang, Y. (2018). Magnitude and pathways of increased nitrous oxide emissions from uplands following permafrost thaw. *Environmental Science & Technology*, 52(16), 9162–9169. https://doi.org/10.1021/acs.est.8b02271
- Yang, G., Peng, Y., Olefeldt, D., Chen, Y., Wang, G., Li, F., Zhang, D., Wang, J., Yu, J., Liu, L., Qin, S., Sun, T., & Yang, Y. (2018). Changes in methane flux along a permafrost thaw sequence on the Tibetan Plateau. Environmental Science & Technology, 52(3), 1244–1252. https://doi.org/10.1021/acs.est.7b04979

#### SUPPORTING INFORMATION

Additional supporting information may be found online in the Supporting Information section.

How to cite this article: Yang, G., Peng, Y., Abbott, B. W., Biasi, C., Wei, B., Zhang, D., Wang, J., Yu, J., Li, F., Wang, G., Kou, D., Liu, F., & Yang, Y. (2021). Phosphorus rather than nitrogen regulates ecosystem carbon dynamics after permafrost thaw. *Global Change Biology*, 27, 5818–5830. <a href="https://doi.org/10.1111/gcb.15845">https://doi.org/10.1111/gcb.15845</a>